

1-1-2017

Sustained Nitric Oxide-Releasing Nanoparticles Interfere with Methicillin-Resistant *Staphylococcus aureus* Adhesion and Biofilm Formation in a Rat Central Venous Catheter Model.

Mircea Radu Mihiu

Vitor Cabral

Rodney Pattabhi

Moses T Tar

Kelvin P Davies

See next page for additional authors

Follow this and additional works at: https://hsrc.himmelfarb.gwu.edu/smhs_derm_facpubs

 Part of the [Dermatology Commons](#)

APA Citation

Mihu, M., Cabral, V., Pattabhi, R., Tar, M., Davies, K., Friedman, A., Martinez, L., & Nosanchuk, J. (2017). Sustained Nitric Oxide-Releasing Nanoparticles Interfere with Methicillin-Resistant *Staphylococcus aureus* Adhesion and Biofilm Formation in a Rat Central Venous Catheter Model.. *Antimicrobial Agents and Chemotherapy*, 61 (1). <http://dx.doi.org/10.1128/AAC.02020-16>

This Journal Article is brought to you for free and open access by the Dermatology at Health Sciences Research Commons. It has been accepted for inclusion in Dermatology Faculty Publications by an authorized administrator of Health Sciences Research Commons. For more information, please contact hsrc@gwu.edu.

Authors

Mircea Radu Mihi, Vitor Cabral, Rodney Pattabhi, Moses T Tar, Kelvin P Davies, Adam J Friedman, Luis R Martinez, and Joshua D Nosanchuk



Sustained Nitric Oxide-Releasing Nanoparticles Interfere with Methicillin-Resistant *Staphylococcus aureus* Adhesion and Biofilm Formation in a Rat Central Venous Catheter Model

Mircea Radu Mihu,^a Vitor Cabral,^{b,c} Rodney Patabhi,^d Moses T. Tar,^e Kelvin P. Davies,^e Adam J. Friedman,^g Luis R. Martinez,^{b,f} Joshua D. Nosanchuk^{b,c}

Department of Medicine, Division of Critical Care, St. Anthony Hospital, Oklahoma City, Oklahoma, USA^a; Department of Medicine, Division of Infectious Diseases,^b and Department of Microbiology and Immunology,^c Albert Einstein College of Medicine and Montefiore Medical Center, Bronx, New York, USA; Department of Medicine, Griffin Hospital, Derby, Connecticut, USA^d; Department of Urology, Albert Einstein College of Medicine, Bronx, New York, USA^e; Department of Biomedical Sciences, NYIT College of Osteopathic Medicine, New York Institute of Technology, Old Westbury, New York, USA^f; Department of Dermatology, George Washington University School of Medicine and Health Sciences, Washington, DC, USA^g

ABSTRACT *Staphylococcus aureus* is frequently isolated in the setting of infections of indwelling medical devices, which are mediated by the microbe's ability to form biofilms on a variety of surfaces. Biofilm-embedded bacteria are more resistant to antimicrobial agents than their planktonic counterparts and often cause chronic infections and sepsis, particularly in patients with prolonged hospitalizations. In this study, we demonstrate that sustained nitric oxide-releasing nanoparticles (NO-np) interfere with *S. aureus* adhesion and prevent biofilm formation on a rat central venous catheter (CVC) model of infection. Confocal and scanning electron microscopy showed that NO-np-treated staphylococcal biofilms displayed considerably reduced thicknesses and bacterial numbers compared to those of control biofilms *in vitro* and *in vivo*, respectively. Although both phenotypes, planktonic and biofilm-associated staphylococci, of multiple clinical strains were susceptible to NO-np, bacteria within biofilms were more resistant to killing than their planktonic counterparts. Furthermore, chitosan, a biopolymer found in the exoskeleton of crustaceans and structurally integrated into the nanoparticles, seems to add considerable antimicrobial activity to the technology. Our findings suggest promising development and translational potential of NO-np for use as a prophylactic or therapeutic against bacterial biofilms on CVCs and other medical devices.

KEYWORDS antimicrobials, biofilms, nanoparticles, nitric oxide, *Staphylococcus aureus*

Staphylococcus aureus is a Gram-positive bacterium that commonly colonizes human nasal membranes and skin. Methicillin-resistant *S. aureus* (MRSA) was first described in 1961 (1), and its prevalence has gradually increased within the population, currently representing a major cause of both community- and health care-associated infections, resulting in high morbidity and mortality (2). Although *S. aureus* is primarily acknowledged for its acute pathogenic characteristics, the microorganism's capacity to cause chronic infections of host tissues or medical implants is based on its ability to adhere to different types of surfaces and form biofilms (3–5). In particular, device-related infections (e.g., related to central venous catheters [CVCs], hemodialysis catheters, prosthetic heart valves, cardiac pacemakers, prosthetic joints, and cerebrospinal fluid

Received 16 September 2016 Returned for modification 11 October 2016 Accepted 1 November 2016

Accepted manuscript posted online 7 November 2016

Citation Mihu MR, Cabral V, Patabhi R, Tar MT, Davies KP, Friedman AJ, Martinez LR, Nosanchuk JD. 2017. Sustained nitric oxide-releasing nanoparticles interfere with methicillin-resistant *Staphylococcus aureus* adhesion and biofilm formation in a rat central venous catheter model. Antimicrob Agents Chemother 61:e02020-16. <https://doi.org/10.1128/AAC.02020-16>.

Copyright © 2016 American Society for Microbiology. All Rights Reserved.

Address correspondence to Luis R. Martinez, lmarti13@nyit.edu, or Joshua D. Nosanchuk, josh.nosanchuk@einstein.yu.edu.

M.R.M. and V.C. contributed equally to this work and share the first author designation.

shunts) are difficult to eradicate given that microbial biofilms are surrounded by an exopolymeric matrix (EPM) that confers resistance to the host immune response and antimicrobial drugs (6). Hence, *S. aureus* has emerged as a leading cause of prosthetic device infections (7, 8).

Approximately 250,000 CVC-related infections occur annually in the United States, with an attributable mortality ranging from 12 to 25% in critically ill patients (9). CVCs are a high risk for staphylococcal biofilm-related infection due to the presence of bacteria in the skin and because they are in direct contact with the patient's bloodstream; it is therefore no surprise that this organism is the leading cause of bloodstream infections in the United States (7). MRSA and methicillin-sensitive *S. aureus* (MSSA) cause 7.4% and 4.7%, respectively, of the central line-associated bloodstream infections (10). Current IDSA guidelines for the treatment of catheter-associated *S. aureus* infections advocate for line removal to facilitate more rapid clearance of the bloodstream and better prognosis (11). The health care costs associated with catheter-related MRSA infections are estimated to range between \$6,916 and \$60,000 per patient (12). Moreover, antimicrobial resistance is associated with higher charges, prolonged hospital stays, and increased death rates (13). Consequently, there is a need for innovative strategies to combat *S. aureus* catheter-related infections, especially biofilm-related infections that exacerbate morbidity, resulting in high mortality (7).

Nitric oxide (NO) is a diatomic, lipophilic gaseous molecule with numerous functions, including cellular signaling, vascular modulation and homeostasis, immune function, pro- and anti-inflammatory properties, and both bactericidal and bacteriostatic properties (14, 15). Our group has previously characterized and extensively demonstrated the therapeutic potential of NO generated and delivered by a silicon-based nanoparticle platform (NO-np) for the treatment of diverse infectious diseases, including Gram-positive and -negative bacterial and fungal skin and soft tissue infections (16–20). While a number of NO-donating compounds have emerged, been evaluated *in vitro*, and shown efficacy against biofilm-forming pathogens, many suffer from various limitations ranging from inadequate release capacity to stability and safety concerns (21–25). A defining feature of the NO-np is that it is a true NO generator, not an NO-donating compound with potential cytotoxicity, such as is seen with diazeniumdiolates (21, 25). The nanoparticles uniquely facilitate the formation of NO from nitrite salt through a stable and potent NO intermediate, N_2O_3 nanoparticles. In fact, the simplicity and the stability of the nanoparticles make them a very attractive treatment modality under many conditions, including combat or disaster situations, especially since they have proven efficacy *in vitro* and *in vivo* in animal models against multidrug-resistant bacteria that are exceedingly difficult to treat with currently available antimicrobials (16, 17). Additionally, safety assessments using cell culture (26) and animal (27) models have demonstrated minimal cytotoxicity and no clinical adverse events, respectively.

Several NO-np platforms have been synthesized and used for antibiofilm applications, highlighting the feasibility and importance of developing these technologies to prevent and fight contamination of prosthetic devices (23, 25, 28–30). Here, we used a CVC MRSA biofilm model to study the effectiveness of NO-np in preventing and eradicating MRSA biofilms (31, 32). Our findings strongly suggest that this nanotechnology can potentially be developed and used in the future as a therapeutic agent for the prevention and treatment of catheter-associated MRSA biofilm infections.

RESULTS

NO-np inhibit MRSA 6498 cells. The efficacy of an antimicrobial is dependent on the concentration used, contact time of exposure, and cell's metabolic activity (Fig. 1). The antibacterial effects of increased concentrations of NO-np on planktonic cells of MRSA clinical strain 6498 were assessed in real-time (Fig. 1A). Cellular growth was reduced by 40% after incubation with 2.5 mg/ml of NO-np and by 50% at concentrations of ≥ 5 mg/ml ($P < 0.0001$). We also evaluated the efficacy of NO-np against MRSA 6498 planktonic cells according to their contact time of exposure. NO-np was found to

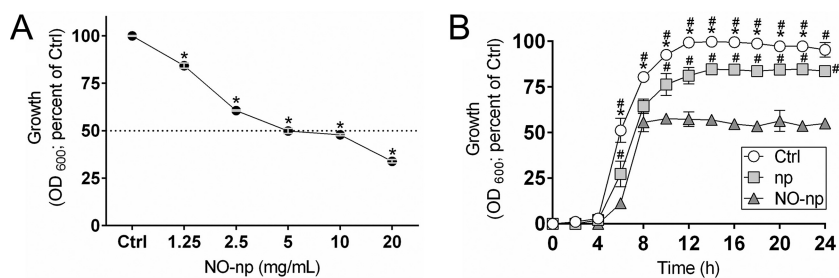


FIG 1 Nitric oxide-releasing nanoparticles (NO-np) inhibit methicillin-resistant *S. aureus* (MRSA) strain 6498 cells. (A) MRSA strain 6498 planktonic cells were grown on polystyrene microtiter plates for 24 h at 37°C in the absence (control; Ctrl) or presence of increasing NO-np (1.25, 2.5, 5, 10, and 20 mg/ml) concentrations. Each point represents the average of three spectrophotometric measurements (optical density at 600 nm [OD₆₀₀]), and error bars indicate standard deviations (SDs). Statistical significance (*, $P < 0.0001$) was calculated by analysis of variance (ANOVA). (B) The effect of NO (5 mg/ml) on MRSA growth kinetics was determined using spectrophotometry (OD₆₀₀) for 24 h. Each symbol represents the average of three measurements for control, np, or NO-np treatment, and error bars indicate SDs. Statistical significance ($P < 0.05$ in comparing the results of control, np, and NO-np treatments) was calculated by multiple *t* tests. *, higher OD compared to np group; #, higher OD compared to NO-np group. (A and B) The initial inoculum was 10^6 staphylococci per well.

be an effective antimicrobial against MRSA strain 6498, with bacterial cell growth substantially reduced after 6 h of exposure ($P < 0.05$) (Fig. 1B). After 8 h of exposure, NO-np reduced cellular growth by 50% compared to the growth of the untreated control, and the reduction remained constant after 24 h ($P < 0.05$). Similarly, bacteria grown in the presence of 5 mg/ml of np demonstrated approximately 20% reduction in microbial growth ($P < 0.05$), strongly suggesting that the chitosan associated with the nanoparticles interferes with MRSA growth (16, 33). Unpublished data in our laboratory using nanoparticles with and without chitosan indicate that 15 to 25% of the total microbial growth inhibition can be attributed to the biopolymer.

NO-np efficacy against *S. aureus* planktonic and biofilm-associated cells. *S. aureus* cells within mature biofilms formed by several strains were significantly more resistant to NO-np than planktonic cells when viability was determined by counting the number of CFU (Fig. 2). On average, the viability of planktonic and biofilm-related bacteria was substantially reduced when biofilms were treated with 1.25 and 2.5 mg/ml of NO-np. However, the viability of cells within biofilms was significantly higher than that of their planktonic counterparts after treatment with similar concentrations of NO-np ($P < 0.05$). Planktonic and biofilm-related cells were killed at significant rates at 5 mg/ml of

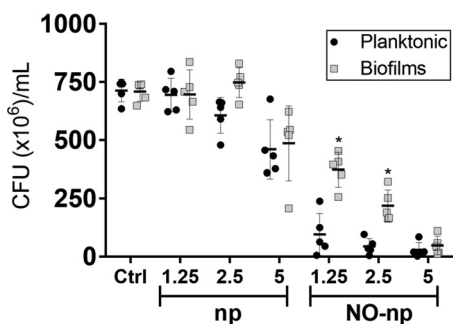


FIG 2 NO-np are effective against *S. aureus* planktonic and biofilm-associated cells. The levels of bacterial viability of six distinct *S. aureus* clinical isolates in biofilms and planktonic cells were determined by CFU counts. Both phenotypes were exposed to 1.25, 2.5, and 5 mg/ml of np or NO-np for 24 h, and their viability was compared to that of bacteria (5×10^6 bacteria per ml) incubated in medium alone. For biofilm formation, the initial inoculum was 10^6 staphylococci per well. The biofilms were allowed to form for 24 h. Each symbol represents the result for a single strain. Black lines are the averages of the results for the six isolates, and error bars denote SDs. Statistical significance (*, $P < 0.05$ in comparing the results for biofilms and planktonic cells) was calculated by multiple *t* tests and adjusted by using the Holm-Sidak method. This experiment was performed twice, with similar results obtained each time.

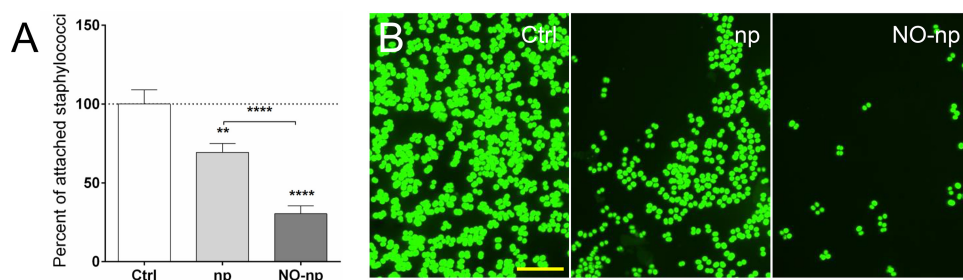


FIG 3 NO-np interferes with adhesion of MRSA strain 6498 to glass-bottom plates. (A) Adhesion to a solid substrate was investigated using poly-D-lysine-coated 35-mm glass-bottom plates and confocal microscopy. Bacteria (10^6 per plate) were allowed to adhere for 90 min in the absence and presence of np or NO-np. After treatment, the plates were rinsed to remove nonadherent cells, attached bacteria were stained with SYTO9 (green fluorescence), images were taken, and the numbers of attached bacteria were counted. Then, the percentage of attached bacteria treated with np or NO-np was calculated relative to the count for the untreated control. Bars represent the averages of five replicates, and error bars denote SDs. Statistical significance (**, $P < 0.01$; ****, $P < 0.0001$) was calculated by ANOVA. (B) Representative images of adhesion by control and np- or NO-np-treated MRSA cells. Scale bar, 10 μm . This experiment was performed twice, with similar results obtained each time.

NO-np. Additionally, both phenotypes showed susceptibility to 5 mg/ml of control np, which suggests that the chitosan incorporated into the nanoparticles may offer some degree of antimicrobial activity, as previously demonstrated (16, 33).

NO-np interferes with adhesion of MRSA strain 6498 to solid substrates. We investigated the ability of MRSA 6498 to adhere to the surface of a glass-bottom plate after NO-np treatment (Fig. 3). NO-np significantly decreased the ability of microbial cells to adhere to glass-bottom plates relative to the adhesion ability of np-treated ($P < 0.0001$) and untreated cells ($P < 0.0001$) (Fig. 3A). Likewise, there was an approximately 30% reduction in adhesion of bacteria incubated with np compared to the adhesion of untreated cells ($P < 0.01$). Confocal microscopy confirmed that np and NO-np affect the interaction of MRSA with the solid substrate compared to the interaction of untreated controls (Fig. 3B), revealing that chitosan plays an important role in the antibiofilm formation efficacy of the nanoparticles (16, 33).

Bacteria within mature biofilms are effectively killed by NO-np. The efficacy of NO-np on MRSA 6498 mature biofilms grown on polystyrene microtiter plates was investigated using both the fluorescein diacetate (FDA) assay and confocal microscopy. Microbial biofilms treated with NO-np showed a significant reduction in cell viability compared to that of the untreated ($P < 0.01$) or np-treated ($P < 0.05$) control (Fig. 4A). For example, the viability of staphylococcal biofilms was reduced 51.8% after treatment with 5 mg/ml of NO-np. Confocal microscopic examination was used to visualize and quantify the effects of NO-np on MRSA 6498 biofilm structure (Fig. 4B to D). Regions of red fluorescence (concanavalin A-Texas Red conjugate) represent EPM (34), and the green fluorescence (SYTO9) indicates bacterial cells (Fig. 4C and D). MRSA biofilms grown in the absence of treatment showed a robust biofilm with homogeneous distribution of bacterial cells and extracellular matrix (Fig. 4C and D). Biofilms exposed to np demonstrated a thickness similar to that of the untreated control ($P < 0.01$) (Fig. 4B), with widespread areas consisting of clumped matrix (Fig. 4C) mostly located on the top of the structure, and bacteria in the deeper areas of the biofilm (Fig. 4D). However, NO-np-treated biofilms displayed a substantially thinner architecture than control biofilms (Fig. 4B) ($P < 0.01$), with multiple areas consisting of clumps of extracellular matrix (Fig. 4C and D).

NO-np interfere with MRSA strain 6498 biofilm formation *in vitro* and *in vivo*. We assessed the ability of continuously NO-releasing np to inhibit MRSA 6498 biofilm formation on catheters *in vitro* and *in vivo* (Fig. 5). First, and as a proof of principle, we added 5-mm catheters to MRSA 6498 cultures and incubated them for 24 h at 37°C under shaking conditions. We used CFU counts to examine biofilm formation on the catheters in the absence and presence of NO (Fig. 5A). Catheters colonized with bacteria and incubated with NO-np evinced significantly lower cell mass than did

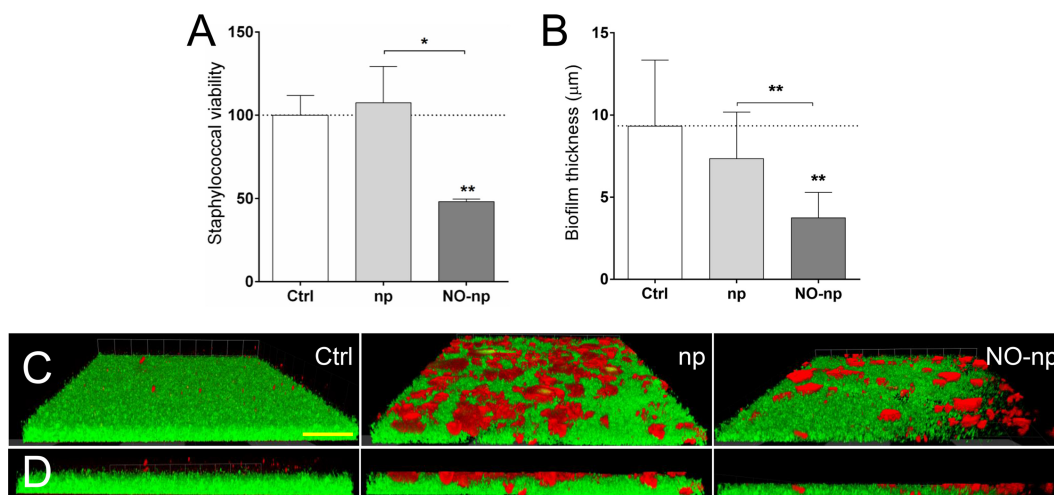


FIG 4 MRSA 6498 cells within mature biofilms are effectively killed by NO-np. Microbial biofilms were grown on polystyrene microtiter or glass-bottom plates for 24 h at 37°C and incubated in the absence and presence of np or NO-np. For biofilm formation, the initial inoculum was 10⁶ MRSA cells per plate. (A) The viability (percentage of control) of biofilm-associated cells was evaluated using the FDA assay. (B) The differences in biofilm thicknesses were examined after exposure to np or NO-np and compared with the biofilm thickness of the untreated control. (A and B) Bars represent the average results from three wells, and error bars denote SDs. Statistical significance (*, *P* < 0.05; **, *P* < 0.01) was calculated by ANOVA. (C) Confocal microscopy of MRSA 6498 strain biofilms after treatment with NO-np. Images of mature bacterial biofilms showed exopolymeric matrix (red; stained with concanavalin A-Texas Red conjugate) and bacterial cells (green; stained with SYTO9). Images were obtained after 24-h coincubation of the bacterial cells in the absence and presence of np or NO-np. (D) The thickness and morphology of each biofilm can be observed in the Z-stack reconstruction. The pictures were taken at a magnification of ×100. (C and D) Scale bar represents 20 µm for all images. (A to D) These experiments were performed twice, with similar results obtained each time.

control catheters (*P* < 0.05). To confirm the results obtained by CFU counts, we utilized the FDA assay and observed that NO-np treatment significantly reduced biofilm-associated cell viability relative to that of untreated (*P* < 0.001) and np-treated (*P* < 0.05) bacteria (Fig. 5B). The slight reduction observed in the viability of bacteria grown

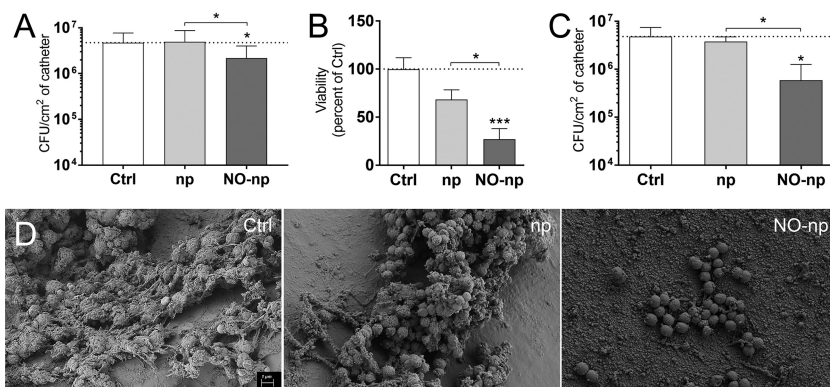


FIG 5 NO-np prevent MRSA strain 6498 biofilm formation in central venous catheters (CVCs) implanted in rats. MRSA biofilms were grown *in vitro* using catheter material as a substrate for 24 h at 37°C and then treated with 5 mg/ml of np or NO-np and compared to untreated controls. For biofilm formation, the initial inoculum was 10⁶ MRSA cells per plate. The microbial mass and viability of biofilm-associated cells were evaluated using the CFU (A) and FDA (B) assays. (A and B) Bars represent the average results from three catheters, and error bars denote SDs. Statistical significance (*, *P* < 0.05; ***, *P* < 0.001) was calculated by ANOVA. These experiments were performed twice, with similar results obtained each time. (C) Mean bacterial burdens in *in vivo* catheters incubated with 10⁶ MRSA cells/ml for 48 h are shown. CVCs implanted in the animals were treated with 5 mg/ml of np or NO-np at 24 h postinfection. This experiment was performed once using three animals (average results from three 5-mm pieces of each catheter per rat) per group. In addition, statistical significance (*, *P* < 0.05) was calculated using ANOVA. Bars represent the average results from three catheters, and error bars denote SDs. (D) Scanning electron microscopy (SEM) examination of MRSA strain biofilm formation on catheters placed in the jugular vein of a Sprague-Dawley rat and treated with PBS or 5 mg/ml of np or NO-np. Scale bar represents 1 µm for all images.

with np is most likely due to the effect of the np on the metabolic activity of the microbial cells. Furthermore, we used a validated rodent CVC model to simulate device-associated infection to define whether NO-np would interfere with MRSA 6498 biofilm formation *in vivo* (Fig. 5C and D) (28, 31, 35, 36). We found significant variations in bacterial burden between catheters treated with NO-np and untreated ($P < 0.01$) or np-treated ($P < 0.05$) catheters (Fig. 5C). Scanning electron microscopy (SEM) images of the luminal surface of untreated control, np-treated, and NO-np-treated catheters were taken 48 h after inoculation with MRSA (Fig. 5D). Untreated catheters demonstrated abundant staphylococcal biofilms that consisted of bacteria embedded in vast amounts of EPM, whereas biofilms formed on np-treated catheters were comprised of clusters of microbial cells interconnected by polysaccharide and surrounded by dispersed EPM. In contrast, catheters treated with NO-np displayed low numbers of bacterial cells and an absence of EPM.

DISCUSSION

S. aureus is the most frequent bacterial pathogen in both hospital- and community-acquired infections (23.6% and 23.7%, respectively) (37). Catheter-associated *S. aureus* infection is a severe health care-acquired disease that may result in septic thrombosis, peripheral abscesses, endocarditis, and death (38). Independent risk factors associated with catheter-related infections include prolonged hospitalization before catheterization, length of catheterization, high bacterial load at the insertion site or on the catheter hub, internal jugular catheterization, and substandard care of the catheter by the health care personnel (39). CVCs are an important source of the sepsis that often affects patients in intensive care units, resulting in prolonged hospitalizations and, possibly, death (40). In this report, we examined the efficacy of NO-np in an MRSA infection model using CVCs inserted into rats. Our findings show that NO-np may reduce CVC microbial colonization by inhibiting bacterial adhesion to the catheter surface. Similarly, we used *in vitro* experiments to demonstrate that this platform is efficacious against mature MRSA biofilms.

Both planktonic and biofilm-associated bacteria were susceptible to NO-np. MRSA cells within biofilms were less susceptible to NO than their planktonic counterparts. It is possible that the absence of EPM in planktonic cells make them more vulnerable and accessible to the antimicrobial effects of NO-np. These results correlate with those presented in other reports that have suggested that the biofilm phenotype shields bacteria within its architecture, conferring resistance to antimicrobial therapy (41, 42). In this regard, pathogenic bacteria are capable of persisting in a biofilm in the presence of antibiotics at levels that are 1,000-fold higher than those necessary to eradicate a planktonic population (43). Although we have previously demonstrated that NO-np is more effective against multiple clinical strains of MSSA and MRSA than commonly used antibiotics (16), this level of efficacy has yet to be compared and validated against bacterial biofilms. However, this was outside the scope of the present study. Remarkably, NO-np reduced the viability of biofilm-related bacteria formed by multiple *S. aureus* clinical isolates, suggesting that this gas can penetrate the EPM to deliver its bactericidal properties. Similar levels of NO efficacy against multidrug-resistant bacteria within biofilms using different synthetic compounds (e.g., *N*-diazoniumdiolates [21, 25], nitrosothiols [24], and nitrosyl metal complexes [22]) have been described. However, these studies showed certain limitations, such as the inability to chemically stabilize and release NO in a controlled manner, safety issues, and perhaps most important, not using multiple strains of a specific bacterial genus to address the variability observed from strain to strain in these types of experiments, hindering the possibility that the methods can be exploited in biomedical applications.

NO kills bacteria by several mechanisms (44). It may bind to iron or thiol groups on the proteins and inactivate enzymes responsible for replication. NO also binds with the superoxide radical O_2^- to form peroxynitrite ($OONO^-$). This species is a strong oxidant and catalyzes membrane lipid peroxidation and the formation of nitrotyrosine residues in proteins. NO will also react with oxygen to form toxic species, such as NO_2 and N_2O_3 .

In this regard, transmission electron microscopy, performed in our laboratory, of MRSA exposed to NO-np revealed cell wall damage and lysis (16). Likewise, chitosan, a polymer naturally found in the exoskeleton of crustaceans and integrated into the nanoparticles, has the advantage of adding significant antimicrobial activity to the technology and is adaptable enough to be combined with other treatments (36, 45–47). For example, chitosan reduced the infection rate of experimentally induced *S. aureus* osteomyelitis in rabbits, thus providing a flexible, biocompatible platform for the design of coatings to protect surfaces from infection (48). Furthermore, this biopolymer enhances the efficacy of antibiotics against Gram-positive and Gram-negative bacteria (49, 50).

S. aureus biofilm formation is a multifactorial process that progresses through coordinated phases. Particularly important is the early growth phase, when the bacterium strongly attaches to a substrate, which is mediated by cell surface factors that may include autolysin (51), teichoic acids (52), or polysaccharide intercellular adhesin (PIA), the product of the *ica* gene (53), whose expression promotes colonization and biofilm formation, especially during environmental stress (54, 55) and in the course of a device-related infection (56). We found that np and NO-np significantly inhibited bacterial adhesion to plastic and glass surfaces. Exposure to nitrosative stress has previously been shown to inhibit *S. aureus* biofilm formation by downregulating the production of PIA (57). Given that np also affect bacterial adhesion, it is possible that chitosan, a cationic biopolymer, alters cell-cell or cell-substrate interactions to prevent biofilm formation (46). Microarray analysis after incubation of *S. aureus* with the acidified-nitrite derivative NO revealed that genes involved in DNA repair, detoxification of reactive oxygen and nitrogen species, and iron regulation are globally induced, providing a plausible explanation for the efficacy of NO-np against preformed biofilms (57).

In summary, we demonstrated that NO-np have antimicrobial activity against *S. aureus* biofilm-related cells. In addition, preformed staphylococcal biofilms were susceptible to NO. MRSA catheter-associated infections are problematic and require periodic removal of infected devices, particularly if severe sepsis, suppurative thrombophlebitis, endocarditis, and bloodstream infection continue. It is possible to treat MRSA biofilm-infected catheters *in situ* by local administration of NO-np alone or in combination with antibiotics (58); alternatively, as NO-np alone or in combination with antibiotics may have a role in preventing biofilm formation, a prophylactic dose may be administered immediately after insertion of the device or incorporated into the catheter material (59). NO-np has shown synergistic efficacy against *Candida albicans* biofilms when used in combination with established antifungal drug therapies *in vitro* (28). One can anticipate that NO, a gas to which microbes develop minimal resistance even following repeated exposures (60), may contribute to the efficacy of drugs to which microorganisms within biofilms have resistance. Additionally, this nanotechnology is a flexible platform to encapsulate antimicrobial drugs for local delivery into infected catheters in order to prevent biofilm formation or eradicate mature biofilms (61). Together, these findings underscore the clear translational potential for the utilization of NO-np in the prevention and treatment of biofilms infecting medical prosthetic devices.

MATERIALS AND METHODS

S. aureus. *S. aureus* isolates were collected, typed, and stored according to an approved protocol at the Albert Einstein College of Medicine (Einstein) and Montefiore Medical Center. A total of six *S. aureus* clinical isolates (strains 38, 67, 85, 112, 132, and 6498) were used in this study. The characteristics of each strain have been described previously (62). The MRSA 6498 isolate used in the majority of the experiments in this report is a USA300 strain collected from a patient's wound and has been utilized extensively in prior work (16, 17). The strains were stored at -80°C in brain heart infusion (BHI) broth with 40% glycerol until use. Test organisms were grown in tryptic soy broth (TSB; MP Biomedicals, LLC) overnight at 37°C on a rotary shaker (Thermo Fisher Scientific) set at 150 rpm. Growth was monitored by measuring the optical density at 600 nm and by using a microtiter plate reader (Bio-Tek).

Synthesis of NO-np and NO release. A hydrogel-glass composite was synthesized using a mixture of tetramethylorthosilicate, polyethylene glycol, chitosan, glucose, and sodium nitrite in a 0.5 mM

sodium phosphate buffer (pH 7) as described previously (26). The nitrite was reduced to NO within the matrix because the glass properties of the composite effected redox reactions initiated with thermally generated electrons from glucose. After the redox reaction, the ingredients were combined and dried using a lyophilizer, resulting in a fine powder comprising nanoparticles containing NO. Once exposed to an aqueous environment, the hydrogel properties of the composite allow for the opening of the water channels inside the particles, facilitating the release of the trapped NO over extended time periods. NO released from the nanoparticles was determined by amperometric detection using the Apollo 4000 nitric oxide detector (World Precision Instruments Ltd.) as previously described (16). The observed trace has been described previously and indicates a relatively stable rate of NO release, with only a slight initial peak (5.64×10^{-6} $\mu\text{g/ml}$ or 18.75 nM) at 70 min (16, 28). A steady-state level (3.76×10^{-6} $\mu\text{g/ml}$ or 12.5 nM) is achieved after 6 h, with continuous release occurring over ~ 24 h. Nanoparticles lacking NO were also produced to serve as controls.

Biofilm formation and NO-np treatment. For each strain, 100 μl of a suspension with 10^6 bacterial cells in BHI medium supplemented with 1% glucose was added into individual wells of polystyrene 96-well plates or poly-D-lysine 35-mm glass-bottom plates (MatTek), and the plates were incubated at 37°C without shaking. The biofilms were allowed to form for 24 h. Biofilms were rinsed 3 times with phosphate-buffered saline (PBS) to remove nonadherent bacteria, and 100 μl of fresh medium without (control) or with 5 mg/ml of NO-np or np alone was added.

Comparison of levels of biofilm and planktonic staphylococcal cell susceptibility to NO-np. *S. aureus* biofilms were incubated with 200 μl of BHI (1% glucose) containing 1.25, 2.5, or 5 mg/ml of np or NO-np. Untreated biofilms were used as a control. *S. aureus* planktonic cells were suspended at a density of 5×10^6 cells per ml in medium alone or in the presence of either np or NO-np. Either *S. aureus* biofilms or planktonic cells were mixed with np or NO-np for 1 min, using a microtiter plate reader mixer to ensure a uniform distribution of the nanoparticles, and were incubated at 37°C for 24 h. CFU counts in killing assays were used to determine the microbial mass.

Killing assay. The toxicity of NO-np for *S. aureus* planktonic cells or within biofilms was evaluated by the CFU count in a killing assay. After incubation with NO-np, biofilms were scraped from the bottom of the wells with a sterile 200- μl micropipette tip and sonicated for 1 min to separate individual staphylococci. Amounts of 100 μl of suspensions containing dissociated cells were aspirated from the wells, transferred to a microcentrifuge tube with 900 μl of PBS, and sonicated again for 1 min. A series of dilutions were then performed, and 100 μl of diluted suspension was plated on BHI (1% glucose) agar plates.

Adherence assay. *S. aureus* cells were incubated on 35-mm glass-bottom dishes with 2 ml of BHI (1% glucose) for 90 min in the absence and presence of 5 mg/ml of np or NO-np. After treatment, the medium was removed, the plates were rinsed once with Hanks' balanced salt solution (HBSS; Sigma), and 200 μl containing 6.6 μM SYTO9 in distilled water (500-nm excitation wavelength and 535-nm emission wavelength; Thermo Fisher Scientific) was added. After 30 min of incubation, the plates containing adhered cells were rinsed once to remove the staining solution, 2 ml of HBSS was added, and confocal images were taken using a Leica TCS SP5 microscope (Wetzlar, Germany) and analyzed using Volocity 3D Image Analysis software (PerkinElmer). As negative controls, plates were incubated with np or NO-np alone. Two independent experiments were performed using multiple replicates.

In vitro catheter biofilm formation assay. Five-millimeter-long catheters were inoculated with *S. aureus* using a 23-gauge needle and incubated in 6-well plates with 1 ml of BHI with 1% glucose at 37°C for 24 h in a rotary shaker. Biofilms were rinsed 3 times with PBS to remove nonbiofilm bacteria, and 100 μl of fresh medium without (control) or with 5 mg/ml of np or NO-np was added and similarly incubated for 24 h. Then, catheters containing biofilms were rinsed once with PBS and the toxicity of NO-np was evaluated using CFU and fluorescein diacetate (FDA; Sigma) assays.

FDA assay. FDA was dissolved in acetone (Sigma) to a concentration of 2 mg/ml, and the solution was stored at -20°C as described previously (63). Subsequently, 100 μl of the solution, prepared by diluting the stock solution 1:50 in PBS, was added to each well. The plates were incubated at 37°C for 1 h on a shaker in the dark. The fluorescence in the wells was measured using a microtiter plate reader equipped with excitation and emission filters of 485 and 535 nm, respectively.

Biofilm architecture. The thicknesses and structural integrity of untreated biofilms and np- or NO-np-treated biofilms were examined using confocal microscopy. Briefly, MRSA biofilms were grown for 24 h in 35-mm glass-bottom culture dishes in the absence or presence of np alone or NO-np, rinsed three times with HBSS, and incubated for 30 min at room temperature in 2 ml of HBSS containing the fluorescent stains SYTO9 (6.6 μM) and concanavalin A-Texas Red conjugate (6.6 μM) with protection from light. The dishes were then rinsed three times with HBSS to remove excess stain. SYTO9 labels bacteria, while concanavalin A-Texas Red conjugate (596-nm excitation wavelength and 615-nm emission wavelength) stains the EPM. Microscopic examinations of biofilms formed in culture plates were performed with confocal microscopy. Two independent experiments were performed using multiple replicates.

In vivo CVC rat model for biofilm formation. A CVC biofilm model was used for *in vivo* experiments, as described elsewhere (31, 35, 36). All animal studies were conducted according to the experimental practices and standards approved by the Institutional Animal Care and Use Committee at Einstein. Briefly, female Sprague-Dawley rats weighing 400 g (Charles Rivers) were anesthetized (3 to 4% isoflurane for induction and 2.0% for maintenance during surgery), and the right external jugular was exposed. A longitudinal incision was made in the vein wall, and a sterile, heparinized (100 U/ml) polyethylene catheter (PE 100 [inner diameter, 0.76 mm; outer diameter, 1.52 mm]; BD) was inserted at a site above the right atrium (~ 2 cm) and secured with 3-0 silk ties. The proximal end of the catheter was tunneled subcutaneously and secured on the subscapular skin by means of a button secured with a 2-0 Ti-Cron

suture. The wound was closed with staples (Ethicon Endo-Surgery). After surgery, a single inoculum of 10^6 bacteria/ml was suspended in 100 μ l of PBS and instilled in the catheter lumen. Twenty-four hours later, a single dose of 5 mg/ml of np or NO-np suspended in 200 μ l was instilled by injection in the catheter lumen ("catheter lock therapy"). Finally, catheters were collected 48 h after infection, cut longitudinally and transected lengthwise (3 animals per group), transferred to a microcentrifuge tube containing 2 ml of PBS, and sonicated for 1 min to detach adherent cells. Serial dilutions of the cell suspensions were performed, and bacteria quantified by the CFU killing assay. This experiment was performed once using three animals (average of three 5-mm pieces of each catheter per rat) per group.

SEM. To assess biofilm formation *in vivo*, SEM was used to examine the catheters of control, np, and NO-np-treated animals as previously described (28). The catheters were transected lengthwise, fixed overnight (4% formaldehyde and 1% glutaraldehyde in PBS), rinsed for 5 min in PBS, and placed in 1% osmium tetroxide for 30 min. After a series of alcohol washes, the samples were critical-point dried (Samdri-790; Tousimis), mounted, coated with gold (Desk-1; Denton Vacuum, Inc.), and viewed in a JEOL JSM-6400 scanning electron microscope in high-vacuum mode at 10 kV.

Statistical analysis. Statistical analyses were performed with GraphPad Prism 6.0 (GraphPad Software, La Jolla, CA) software. Analyses of kinetics, adhesion, CFU, FDA, and biofilm thickness determinations were done using analysis of variance (ANOVA). Biofilm and planktonic cell comparisons were calculated by multiple *t* tests and adjusted by using the Holm-Sidak method. *P* values of < 0.05 were considered significant.

ACKNOWLEDGMENTS

L.R.M. was supported by the National Institute of General Medical Sciences of the U.S. NIH under award number R15GM117501 and NYIT College of Osteopathic Medicine intramural funds.

M.R.M., V.C., R.P., M.T.T., K.P.D., and L.R.M. declare no conflict of interest. A.J.F. is a coinventor of the NO-np platform. A.J.F. and J.D.N. serve as advisors for Nano BioMed, Inc.

REFERENCES

- Barber M. 1961. Methicillin-resistant staphylococci. *J Clin Pathol* 14: 385–393. <https://doi.org/10.1136/jcp.14.4.385>.
- Klein E, Smith DL, Laxminarayan R. 2007. Hospitalizations and deaths caused by methicillin-resistant *Staphylococcus aureus*, United States, 1999–2005. *Emerg Infect Dis* 13:1840–1846. <https://doi.org/10.3201/eid1312.070629>.
- Kiedrowski MR, Horswill AR. 2011. New approaches for treating staphylococcal biofilm infections. *Ann N Y Acad Sci* 1241:104–121. <https://doi.org/10.1111/j.1749-6632.2011.06281.x>.
- Gotz F. 2002. Staphylococcus and biofilms. *Mol Microbiol* 43:1367–1378. <https://doi.org/10.1046/j.1365-2958.2002.02827.x>.
- Parsek MR, Singh PK. 2003. Bacterial biofilms: an emerging link to disease pathogenesis. *Annu Rev Microbiol* 57:677–701. <https://doi.org/10.1146/annurev.micro.57.030502.090720>.
- O'Gara JP, Humphreys H. 2001. Staphylococcus epidermidis biofilms: importance and implications. *J Med Microbiol* 50:582–587. <https://doi.org/10.1099/0022-1317-50-7-582>.
- Wisplinghoff H, Bischoff T, Tallent SM, Seifert H, Wenzel RP, Edmond MB. 2004. Nosocomial bloodstream infections in US hospitals: analysis of 24,179 cases from a prospective nationwide surveillance study. *Clin Infect Dis* 39:309–317. <https://doi.org/10.1086/421946>.
- Fowler VG, Jr, Miro JM, Hoen B, Cabell CH, Abrutyn E, Rubinstein E, Corey GR, Spelman D, Bradley SF, Barsic B, Pappas PA, Anstrom KJ, Wray D, Fortes CQ, Anguera I, Athan E, Jones P, van der Meer JT, Elliott TS, Levine DP, Bayer AS, Investigators ICE. 2005. Staphylococcus aureus endocarditis: a consequence of medical progress. *JAMA* 293:3012–3021. <https://doi.org/10.1001/jama.293.24.3012>.
- Khanna V, Mukhopadhyay C, Eshwara VK, Verma M, Dabke P. 2013. Evaluation of central venous catheter associated blood stream infections: a microbiological observational study. *J Pathog* 2013:936864. <https://doi.org/10.1155/2013/936864>.
- Burton DC, Edwards JR, Horan TC, Jernigan JA, Fridkin SK. 2009. Methicillin-resistant Staphylococcus aureus central line-associated bloodstream infections in US intensive care units, 1997–2007. *JAMA* 301:727–736. <https://doi.org/10.1001/jama.2009.153>.
- Mermel LA, Allon M, Bouza E, Craven DE, Flynn P, O'Grady NP, Raad II, Rijnders BJ, Sherertz RJ, Warren DK. 2009. Clinical practice guidelines for the diagnosis and management of intravascular catheter-related infection: 2009 update by the Infectious Diseases Society of America. *Clin Infect Dis* 49:1–45. <https://doi.org/10.1086/599376>.
- Nakamura I, Fukushima S, Hayakawa T, Sekiya K, Matsumoto T. 2015. The additional costs of catheter-related bloodstream infections in intensive care units. *Am J Infect Control* 43:1046–1049. <https://doi.org/10.1016/j.ajic.2015.05.022>.
- Neidell MJ, Cohen B, Furuya Y, Hill J, Jeon CY, Glied S, Larson EL. 2012. Costs of healthcare- and community-associated infections with antimicrobial-resistant versus antimicrobial-susceptible organisms. *Clin Infect Dis* 55:807–815. <https://doi.org/10.1093/cid/cis552>.
- Friedman A, Friedman J. 2009. New biomaterials for the sustained release of nitric oxide: past, present and future. *Expert Opin Drug Deliv* 6:1113–1122. <https://doi.org/10.1517/17425240903196743>.
- De Groote MA, Fang FC. 1995. NO inhibitions: antimicrobial properties of nitric oxide. *Clin Infect Dis* 21(Suppl 2):S162–S165. https://doi.org/10.1093/clinids/21.Supplement_2.S162.
- Martinez LR, Han G, Chacko M, Mihi MR, Jacobson M, Gialanella P, Friedman AJ, Nosanchuk JD, Friedman JM. 2009. Antimicrobial and healing efficacy of sustained release nitric oxide nanoparticles against *Staphylococcus aureus* skin infection. *J Invest Dermatol* 129:2463–2469. <https://doi.org/10.1038/jid.2009.95>.
- Han G, Martinez LR, Mihi MR, Friedman AJ, Friedman JM, Nosanchuk JD. 2009. Nitric oxide releasing nanoparticles are therapeutic for Staphylococcus aureus abscesses in a murine model of infection. *PLoS One* 4:e7804. <https://doi.org/10.1371/journal.pone.0007804>.
- Macherla C, Sanchez DA, Ahmadi MS, Vellozzi EM, Friedman AJ, Nosanchuk JD, Martinez LR. 2012. Nitric oxide releasing nanoparticles for treatment of *Candida albicans* burn infections. *Front Microbiol* 3:193. <https://doi.org/10.3389/fmicb.2012.00193>.
- Mihi MR, Sandkovsky U, Han G, Friedman JM, Nosanchuk JD, Martinez LR. 2010. The use of nitric oxide releasing nanoparticles as a treatment against *Acinetobacter baumannii* in wound infections. *Virulence* 1:62–67. <https://doi.org/10.4161/viru.1.2.10038>.
- Friedman A, Blecher K, Sanchez D, Tuckman-Vernon C, Gialanella P, Friedman JM, Martinez LR, Nosanchuk JD. 2011. Susceptibility of Gram-positive and -negative bacteria to novel nitric oxide-releasing nanoparticle technology. *Virulence* 2:217–221. <https://doi.org/10.4161/viru.2.3.16161>.
- Duong HT, Jung K, Kutty SK, Agustina S, Adnan NN, Basuki JS, Kumar N, Davis TP, Barraud N, Boyer C. 2014. Nanoparticle (star polymer) delivery of nitric oxide effectively negates *Pseudomonas aeruginosa* biofilm formation. *Biomacromolecules* 15:2583–2589. <https://doi.org/10.1021/bm500422v>.
- Halpenny GM, Gandhi KR, Mascharak PK. 2010. Eradication of patho-

- genic bacteria by remote delivery of nitric oxide via light-triggering of nitrosyl-containing materials. *ACS Med Chem Lett* 1:180–183. <https://doi.org/10.1021/ml1000646>.
23. Hetrick EM, Shin JH, Paul HS, Schoenfisch MH. 2009. Anti-biofilm efficacy of nitric oxide-releasing silica nanoparticles. *Biomaterials* 30:2782–2789. <https://doi.org/10.1016/j.biomaterials.2009.01.052>.
 24. Kishikawa H, Ebberyd A, Romling U, Brauner A, Luthje P, Lundberg JO, Weitzberg E. 2013. Control of pathogen growth and biofilm formation using a urinary catheter that releases antimicrobial nitrogen oxides. *Free Radic Biol Med* 65:1257–1264. <https://doi.org/10.1016/j.free-radbiomed.2013.09.012>.
 25. Ren H, Wu J, Colletta A, Meyerhoff ME, Xi C. 2016. Efficient eradication of mature *Pseudomonas aeruginosa* biofilm via controlled delivery of nitric oxide combined with antimicrobial peptide and antibiotics. *Front Microbiol* 7:1260. <https://doi.org/10.3389/fmicb.2016.01260>.
 26. Friedman AJ, Han G, Navati MS, Chacko M, Gunther L, Alfieri A, Friedman JM. 2008. Sustained release nitric oxide releasing nanoparticles: characterization of a novel delivery platform based on nitrite containing hydrogel/glass composites. *Nitric Oxide* 19:12–20. <https://doi.org/10.1016/j.niox.2008.04.003>.
 27. Cabrales P, Han G, Nacharaju P, Friedman AJ, Friedman JM. 2011. Reversal of hemoglobin-induced vasoconstriction with sustained release of nitric oxide. *Am J Physiol Heart Circ Physiol* 300:H49–H56. <https://doi.org/10.1152/ajpheart.00665.2010>.
 28. Ahmadi M, Lee HH, Sanchez DA, Friedman AJ, Tar MT, Davis KP, Nosanchuk JD, Martinez LR. 2016. Sustained nitric oxide releasing nanoparticles induce cell death in *Candida albicans* yeast and hyphal cells, preventing biofilm formation in vitro and in a rodent central venous catheter model. *Antimicrob Agents Chemother* 60:2185–2194. <https://doi.org/10.1128/AAC.02659-15>.
 29. Worley BV, Schilly KM, Schoenfisch MH. 2015. Anti-biofilm efficacy of dual-action nitric oxide-releasing alkyl chain modified poly(amidoamine) dendrimers. *Mol Pharm* 12:1573–1583. <https://doi.org/10.1021/acs.molpharmaceut.5b00006>.
 30. Lu Y, Slomberg DL, Shah A, Schoenfisch MH. 2013. Nitric oxide-releasing amphiphilic poly(amidoamine) (PAMAM) dendrimers as antibacterial agents. *Biomacromolecules* 14:3589–3598. <https://doi.org/10.1021/bm400961r>.
 31. Ulphani JS, Rupp ME. 1999. Model of *Staphylococcus aureus* central venous catheter-associated infection in rats. *Lab Anim Sci* 49:283–287.
 32. Van Praagh AD, Li T, Zhang S, Arya A, Chen L, Zhang XX, Bertolami S, Mortin LI. 2011. Daptomycin antibiotic lock therapy in a rat model of staphylococcal central venous catheter biofilm infections. *Antimicrob Agents Chemother* 55:4081–4089. <https://doi.org/10.1128/AAC.00147-11>.
 33. He M, Lu L, Zhang J, Li D. 2015. Immobilized silver nanoparticles on chitosan with special surface state-enhanced antimicrobial efficacy and reduced cytotoxicity. *J Nanosci Nanotechnol* 15:6435–6443. <https://doi.org/10.1166/jnn.2015.10782>.
 34. Hochbaum AI, Kolodkin-Gal I, Foulston L, Kolter R, Aizenberg J, Losick R. 2011. Inhibitory effects of D-amino acids on *Staphylococcus aureus* biofilm development. *J Bacteriol* 193:5616–5622. <https://doi.org/10.1128/JB.05534-11>.
 35. Andes D, Nett J, Oschel P, Albrecht R, Marchillo K, Pitula A. 2004. Development and characterization of an in vivo central venous catheter *Candida albicans* biofilm model. *Infect Immun* 72:6023–6031. <https://doi.org/10.1128/IAI.72.10.6023-6031.2004>.
 36. Martinez LR, Mihu MR, Tar M, Cordero RJ, Han G, Friedman AJ, Friedman JM, Nosanchuk JD. 2010. Demonstration of antibiofilm and antifungal efficacy of chitosan against candidal biofilms, using an in vivo central venous catheter model. *J Infect Dis* 201:1436–1440. <https://doi.org/10.1086/651558>.
 37. Biedenbach DJ, Moet GJ, Jones RN. 2004. Occurrence and antimicrobial resistance pattern comparisons among bloodstream infection isolates from the SENTRY Antimicrobial Surveillance Program (1997–2002). *Diagn Microbiol Infect Dis* 50:59–69. <https://doi.org/10.1016/j.diagmicrobio.2004.05.003>.
 38. Fowler VG, Jr, Justice A, Moore C, Benjamin DK, Jr, Woods CW, Campbell S, Reller LB, Corey GR, Day NP, Peacock SJ. 2005. Risk factors for hematogenous complications of intravascular catheter-associated *Staphylococcus aureus* bacteremia. *Clin Infect Dis* 40:695–703. <https://doi.org/10.1086/427806>.
 39. Lorente L, Henry C, Martin MM, Jimenez A, Mora ML. 2005. Central venous catheter-related infection in a prospective and observational study of 2,595 catheters. *Crit Care* 9:R631–R635. <https://doi.org/10.1186/cc3824>.
 40. Richards MJ, Edwards JR, Culver DH, Gaynes RP. 1999. Nosocomial infections in medical intensive care units in the United States. National Nosocomial Infections Surveillance System. *Crit Care Med* 27:887–892.
 41. Folkesson A, Haagensen JA, Zampaloni C, Sternberg C, Molin S. 2008. Biofilm induced tolerance towards antimicrobial peptides. *PLoS One* 3:e1891. <https://doi.org/10.1371/journal.pone.0001891>.
 42. Morales M, Mendez-Alvarez S, Martin-Lopez JV, Marrero C, Freytes CO. 2004. Biofilm: the microbial “bunker” for intravascular catheter-related infection. *Support Care Cancer* 12:701–707. <https://doi.org/10.1007/s00520-004-0630-5>.
 43. Cerca N, Martins S, Cerca F, Jefferson KK, Pier GB, Oliveira R, Azeredo J. 2005. Comparative assessment of antibiotic susceptibility of coagulase-negative staphylococci in biofilm versus planktonic culture as assessed by bacterial enumeration or rapid XTT colorimetry. *J Antimicrob Chemother* 56:331–336. <https://doi.org/10.1093/jac/dki217>.
 44. Hurford WE. 2005. Nitric oxide as a bactericidal agent: is the cure worse than the disease? *Respir Care* 50:1428–1429.
 45. Sajomsang W, Tantayanon S, Tangpasuthadol V, Daly WH. 2009. Quaternization of N-aryl chitosan derivatives: synthesis, characterization, and antibacterial activity. *Carbohydr Res* 344:2502–2511. <https://doi.org/10.1016/j.carres.2009.09.004>.
 46. Martinez LR, Mihu MR, Han G, Frases S, Cordero RJ, Casadevall A, Friedman AJ, Friedman JM, Nosanchuk JD. 2010. The use of chitosan to damage *Cryptococcus neoformans* biofilms. *Biomaterials* 31:669–679. <https://doi.org/10.1016/j.biomaterials.2009.09.087>.
 47. Tsai T, Chien HF, Wang TH, Huang CT, Ker YB, Chen CT. 2011. Chitosan augments photodynamic inactivation of gram-positive and gram-negative bacteria. *Antimicrob Agents Chemother* 55:1883–1890. <https://doi.org/10.1128/AAC.00550-10>.
 48. Peng ZX, Tu B, Shen Y, Du L, Wang L, Guo SR, Tang TT. 2011. Quaternized chitosan inhibits icaA transcription and biofilm formation by *Staphylococcus* on a titanium surface. *Antimicrob Agents Chemother* 55:860–866. <https://doi.org/10.1128/AAC.01005-10>.
 49. Hoque J, Adhikary U, Yadav V, Samaddar S, Konai MM, Prakash RG, Paramanandham K, Shome BR, Sanyal K, Halder J. 2016. Chitosan derivatives active against multi-drug-resistant bacteria and pathogenic fungi: in vivo evaluation as topical antimicrobials. *Mol Pharm* 13:3578–3589. <https://doi.org/10.1021/acs.molpharmaceut.6b00764>.
 50. Jamil B, Habib H, Abbasi SA, Ihsan A, Nasir H, Imran M. 2016. Development of cefotaxime impregnated chitosan as nano-antibiotics: de novo strategy to combat biofilm forming multi-drug resistant pathogens. *Front Microbiol* 7:330. <https://doi.org/10.3389/fmicb.2016.00330>.
 51. Biswas R, Voggu L, Simon UK, Hentschel P, Thumm G, Gotz F. 2006. Activity of the major staphylococcal autolysin Atl. *FEMS Microbiol Lett* 259:260–268. <https://doi.org/10.1111/j.1574-6968.2006.00281.x>.
 52. Gross M, Cramton SE, Gotz F, Peschel A. 2001. Key role of teichoic acid net charge in *Staphylococcus aureus* colonization of artificial surfaces. *Infect Immun* 69:3423–3426. <https://doi.org/10.1128/IAI.69.5.3423-3426.2001>.
 53. Heilmann C, Schweitzer O, Gerke C, Vanittanakom N, Mack D, Gotz F. 1996. Molecular basis of intercellular adhesion in the biofilm-forming *Staphylococcus epidermidis*. *Mol Microbiol* 20:1083–1091. <https://doi.org/10.1111/j.1365-2958.1996.tb02548.x>.
 54. Glynn AA, O'Donnell ST, Molony DC, Sheehan E, McCormack DJ, O'Gara JP. 2009. Hydrogen peroxide induced repression of icaADBC transcription and biofilm development in *Staphylococcus epidermidis*. *J Orthop Res* 27:627–630. <https://doi.org/10.1002/jor.20758>.
 55. Formosa-Dague C, Feuillie C, Beaussart A, Derclaye S, Kucharikova S, Lasa I, Van Dijk P, Dufrene YF. 2016. Sticky matrix: adhesion mechanism of the staphylococcal polysaccharide intercellular adhesin. *ACS Nano* 10:3443–3452. <https://doi.org/10.1021/acsnano.5b07515>.
 56. Fluckiger U, Ulrich M, Steinhuber A, Doring G, Mack D, Landmann R, Goerke C, Wolz C. 2005. Biofilm formation, icaADBC transcription, and polysaccharide intercellular adhesin synthesis by staphylococci in a device-related infection model. *Infect Immun* 73:1811–1819. <https://doi.org/10.1128/IAI.73.3.1811-1819.2005>.
 57. Schlag S, Nerz C, Birkenstock TA, Altenberend F, Gotz F. 2007. Inhibition of staphylococcal biofilm formation by nitrite. *J Bacteriol* 189:7911–7919. <https://doi.org/10.1128/JB.00598-07>.
 58. Guzman LA, Labhasetwar V, Song C, Jang Y, Lincoff AM, Levy R, Topol EJ. 1996. Local intraluminal infusion of biodegradable polymeric nanopar-

- ticles. A novel approach for prolonged drug delivery after balloon angioplasty. *Circulation* 94:1441–1448.
59. Evliyaoglu Y, Kobaner M, Celebi H, Yelsel K, Dogan A. 2011. The efficacy of a novel antibacterial hydroxyapatite nanoparticle-coated indwelling urinary catheter in preventing biofilm formation and catheter-associated urinary tract infection in rabbits. *Urol Res* 39:443–449. <https://doi.org/10.1007/s00240-011-0379-5>.
60. Privett BJ, Broadnax AD, Bauman SJ, Riccio DA, Schoenfisch MH. 2012. Examination of bacterial resistance to exogenous nitric oxide. *Nitric Oxide* 26:169–173. <https://doi.org/10.1016/j.niox.2012.02.002>.
61. Sanchez DA, Schairer D, Tuckman-Vernon C, Chouake J, Kutner A, Makdisi J, Friedman JM, Nosanchuk JD, Friedman AJ. 2014. Amphoterin B releasing nanoparticle topical treatment of *Candida* spp. in the setting of a burn wound. *Nanomedicine* 10:269–277. <https://doi.org/10.1016/j.nano.2013.06.002>.
62. Mihiu MR, Roman-Sosa J, Varshney AK, Eugenin EA, Shah BP, Ham Lee H, Nguyen LN, Guimaraes AJ, Fries BC, Nosanchuk JD, Martinez LR. 2015. Methamphetamine alters the antimicrobial efficacy of phagocytic cells during methicillin-resistant *Staphylococcus aureus* skin infection. *mBio* 6:e01622269–15. <https://doi.org/10.1128/mBio.01622-15>.
63. Honraet K, Goetghebeur E, Nelis HJ. 2005. Comparison of three assays for the quantification of *Candida* biomass in suspension and CDC reactor grown biofilms. *J Microbiol Methods* 63:287–295. <https://doi.org/10.1016/j.mimet.2005.03.014>.